

## **Distributed maximum power point tracking in photovoltaic applications: active bypass DC/DC converter**

### **Seguimiento del punto de máxima potencia distribuida en aplicaciones fotovoltaicas: convertidor DC/DC para desviación activa**

*Carlos Andrés Ramos-Paja*<sup>\*1</sup>, *Roberto Giral*<sup>2</sup>, *Eliana Isabel Arango Zuluaga*<sup>1</sup>

<sup>1</sup>Universidad Nacional de Colombia. Carrera 80 N° 65-223. Medellín, Colombia.

<sup>2</sup>Universitat Rovira i Virgili. Avda. Països Catalans 26, 43007. Tarragona, España.

(Recibido el 10 de enero de 2012. Aceptado el 28 de agosto de 2012)

#### **Abstract**

An active bypass structure is proposed to maximize the power production in photovoltaic modules under mismatched conditions. Its efficiency is compared with single and distributed maximum power point tracking solutions based on conventional DC/DC structures. The analysis and simulations performed under realistic assumptions demonstrate the benefits of the novel active bypass converter over solutions based on Boost, Buck or Buck-Boost converters.

----- *Keywords:* Active bypass, efficiency, distributed maximum power point tracking

#### **Resumen**

Se propone una estructura de desvío activo para maximizar la producción de potencia en sistemas fotovoltaicos bajo condiciones irregulares de operación, comparando su eficiencia con soluciones individuales y distribuidas basadas en convertidores DC/DC convencionales. Los análisis y simulaciones realistas demuestran las ventajas del nuevo convertidor de desvío activo sobre soluciones basadas en convertidores Boost, Buck y Buck-Boost.

----- *Palabras clave:* Desviación activa, eficiencia, seguimiento de punto de máxima potencia

---

\* Autor de correspondencia: teléfono: + 57+4+425 53 45, fax: + 57+4+234 10 02, correo electrónico: caramosp@unal.edu.co (C. Ramos)

## Introduction

To improve photovoltaic (PV) generation systems, multiple regulation strategies able to find the optimal PV operating conditions for different solar irradiance and ambient temperature have been proposed, named Maximum Power Point Tracking (MPPT) algorithms [1]. Similarly, circuit structures to mitigate the power reduction caused by mismatching in the PV panels due to shadowing, clouding or modules tolerances, have been designed [2]. Such solutions have been developed to address both stand-alone and grid-connected applications using DC/DC switching converters. In stand-alone applications the DC/DC converter is used to adapt the PV power to the load requirements, while in grid-connected applications there are two typical approaches [2]: single-stage and double-stage (DS) inverters. In the DS structures, which block diagram is presented in figure 1, the PV power is optimized by means of a DC/DC converter, and a DC-link transfers the PV power to the grid-connected or stand-alone inverter.

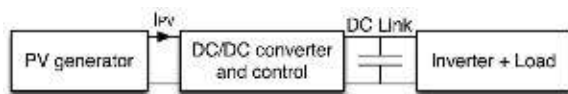


**Figure 1** Double stage PV grid-connected system

In addition, many solutions to overcome the problems of power and voltage reduction caused by PV module mismatching connected to a centralized inverter have been addressed by splitting the PV generator in smaller subfields. In this context, each PV module is associated with either its own MPPT capable DC/AC micro-inverter or DC/DC converter [3], then both solutions coexist, at module level, with the classical diodes that avoid hot spots by bypassing smaller groups of cells in series. The adoption of a dedicated DC/DC converter for each PV panel is known as Distributed Maximum Power Point Tracking (DMPPT) [1], where each PV panel is driven to its optimal operating point. Moreover, almost all grid-connected DS solutions use a DC/

AC inverter with a built-in regulation of the DC-link since it is a commercial standard [4].

This paper is based on the works “Minimizing the effects of shadowing in a PV module by means of active voltage sharing” and “PV field distributed maximum power point tracking by means of an active bypass converter”, developed by the authors, which appeared in the IEEE International Conference on Industrial Technology (ICIT-2010, © 2010 IEEE) and in the International Conference on Clean Electrical Power (ICCEP-2011, © 2011 IEEE), respectively. This paper proposes a new active-bypass solution (AB) to maximize the power extracted from PV panels at a module granularity level [3], [5]. The proposed AB structure uses a parallel-like connection instead of the cascade, series-like, connection of typical DMPPT solutions [3], therefore the AB circuit requires one inductor less than DMPPT based on Boost, Buck or Buck-Boost converters. This structural difference is also important in terms of efficiency since lower losses are present.

To provide comparison with solutions based on single MPPT traditional interfaces, the efficiencies of MPPT approaches based on typical DC/DC converters are analyzed. In addition, an overview on the basic topics related to PV generation systems and the mismatching phenomenon is given, and the basic concepts on DMPPT systems are also discussed. Moreover, the novel AB solution is analyzed in terms of efficiency and DMPPT capability, validating the proposed circuit and control algorithm by means of detailed and realistic simulations based on experimentally validated PV models. Finally, the conclusions of the work are given.

## Typical DC/DC converters for maximum power point tracking

A PV panel can be modeled by using the non-linear approach given in [5], where the PV effect is represented by its electrical equivalent. Figure 2(a) shows the model of a BP585 PV panel.

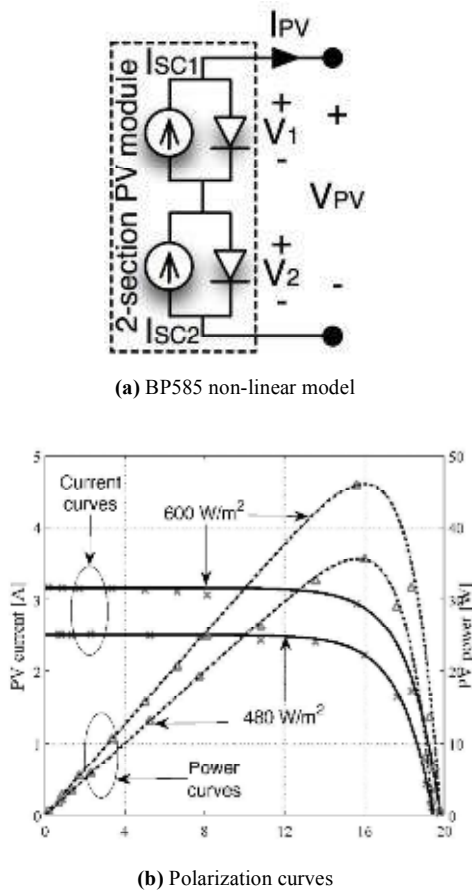


**Figure 2** BP585 model (continuous traces) and experimental (discrete traces) characteristics

From the model of figure 2(a) it is noted that the BP585, as several commercial PV panels, is composed by two PV modules in series to reduce the effect of shadows in the power production, where both modules have almost identical characteristics. Figure 2(b) shows the experimental electrical characteristics of a BP585 operating at 35 °C and at two different irradiance conditions:  $S_{em1} = 600 \text{ W/m}^2$  and  $S_{em2} = 480 \text{ W/m}^2$ . Moreover, the model reported in figure 2(a), and given in (1), was parameterized to reproduce the PV panel experimental behavior, obtaining the model parameters  $A_m = 10^{-5} \text{ A}$  and  $B_m = 0.32 \text{ V}^{-1}$ . The short-circuit current  $I_{SC}$  depends on the irradiance conditions: for  $S_{em1}$ ,  $I_{SC} = 3.16 \text{ A}$ , and for  $S_{em2}$ ,  $I_{SC} = 2.5 \text{ A}$ . Figure 2(b) also presents the model polarization curves as continuous traces, it validating the model accuracy.

$$i_{PV} = I_{SC} - A_m \times \exp(B_m \times v_{PV}) \quad (1)$$

In the experiments, the PV open-circuit voltage  $V_{OC}$  is near to 19 V, and the optimal operating point (MPP), where the maximum PV power is produced, is characterized for a PV voltage between 15 V and 16 V, named  $V_{MPP}$ . Moreover, the PV current at the MPP is named  $I_{MPP}$ .

There are several MPPT strategies to find the MPP [1], where the most adopted one concerns the Perturb and Observe (P&O) technique [2], which modifies the PV voltage in the direction that generates a positive change in the PV power. The P&O flowchart is given in figure 3(a) [1].

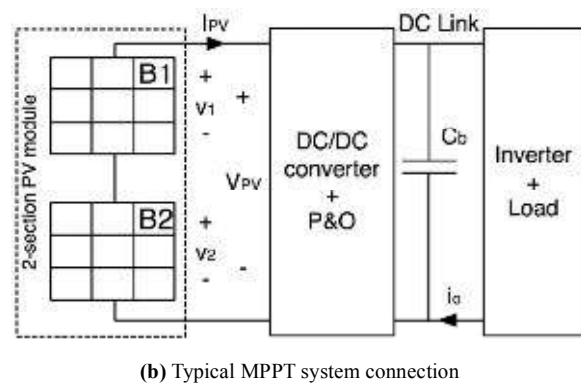
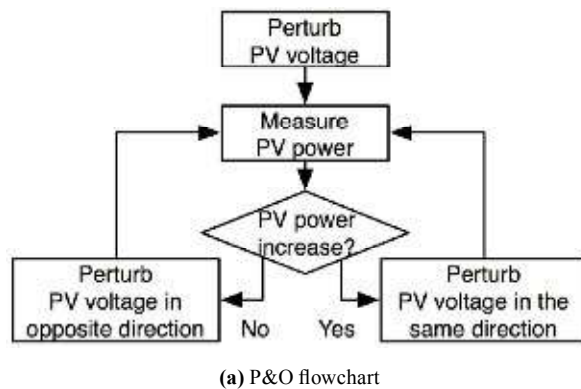


**Figure 3** Typical PV grid-connected scheme for MPPT based on P&O

In addition, figure 3(b) describes the classical scheme for grid-connected PV applications [2] where the DC/DC converter is regulated by means of the P&O algorithm [1, 2, 4].

An important condition to select the DC/DC converter in figure 3(b) is the desired DC-link voltage at the input of the inverter, which regulates the voltage  $V_b$  of the bulk capacitor  $C_b$ . In this way, typical Boost, Buck, and Buck-Boost topologies are widely adopted, but the output voltage of a PV system based on such converters is not the same. Such a condition can be addressed by a proper selection of the inverter, e.g. Buck, Boost, or Buck-Boost inverter. Moreover, a structural reorganization of the PV array can be used to achieve a desired inverter input voltage.

**MPPT based on a Boost converter**

The electrical scheme of the Boost converter based MPPT approach is depicted in figure 4, where a synchronous configuration has been adopted since it provides a higher efficiency than the classical Boost. Such a circuit models the closed-loop inverter by a voltage source, and the parasitic resistances of the inductor and MOSFETs have been collected into the  $R_L$  resistor [6].

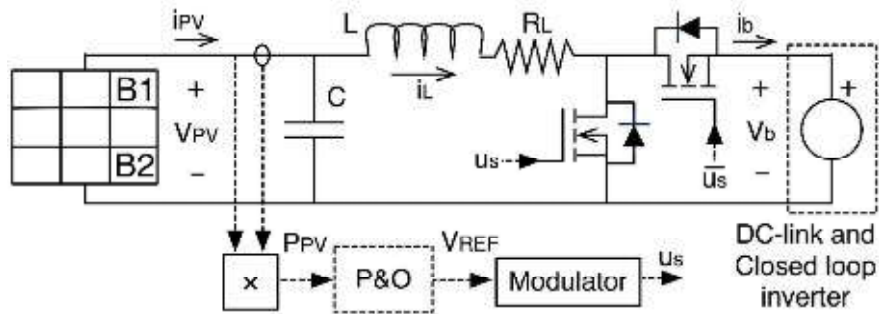


**Figure 4** MPPT system based on a Boost converter

From the steady-state analysis of figure 4 circuit, and considering the PV panel operating at its MPP,  $V_{PV} = V_{MPP}$  and  $I_{PV} = I_{MPP}$ , the inductor current  $i_L$  is given by  $I_{BO} = I_{MPP}$  and the duty cycle  $D_{BO}$  required to operate in such MPP considering a regulated DC-link voltage  $V_b$  is

$$D_{BO} = 1 - \frac{V_{MPP} - I_{MPP} \cdot R_L}{V_b} \quad (2)$$

Then, the power losses on this Boost MPPT approach at the PV panel MPP is calculated as

$$P_{Loss,BO} = I_{MPP}^2 \cdot R_L \quad (3)$$

**MPPT based on a Buck converter**

The Buck converter based MPPT approach is depicted in figure 5, where again a synchronous configuration has been adopted with a single  $R_L$  resistor. From its circuitual steady-state analysis, the inductor current is  $I_{BU} = I_{MPP}/D_{BU}$ , and the duty cycle and power losses at the MPP for this Buck based MPPT approach are given by (4) and (5), respectively.

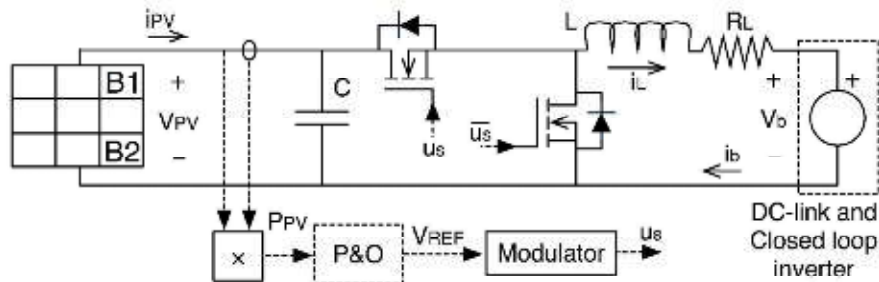


**Figure 5** MPPT system based on a Buck converter

$$D_{BU} = \frac{V_b + \sqrt{V_b^2 + 4 \cdot V_{MPP} \cdot I_{MPP} \cdot R_L}}{2 \cdot V_{MPP}} \quad (4)$$

$$P_{Loss,BU} = \frac{I_{MPP}^2 \cdot R_L}{D_{BU}^2} \quad (5)$$

**MPPT based on a Buck-Boost converter**

The Buck-Boost converter based MPPT approach, based on a non-inverting synchronous

configuration, is depicted in figure 6. From its steady-state analysis, the inductor current at the MPP is  $I_{BB} = I_{MPP}/D_{BB}$ , while the duty cycle  $D_{BB}$  and power losses  $P_{Loss,BB}$  are:

$$D_{BB} = \frac{V_b + \sqrt{V_b^2 + 4 \cdot (V_{MPP} + V_b) \cdot I_{MPP} \cdot R_L}}{2 \cdot (V_{MPP} + V_b)} \quad (6)$$

$$P_{Loss,BB} = \frac{I_{MPP}^2 \cdot R_L}{D_{BB}^2} \quad (7)$$

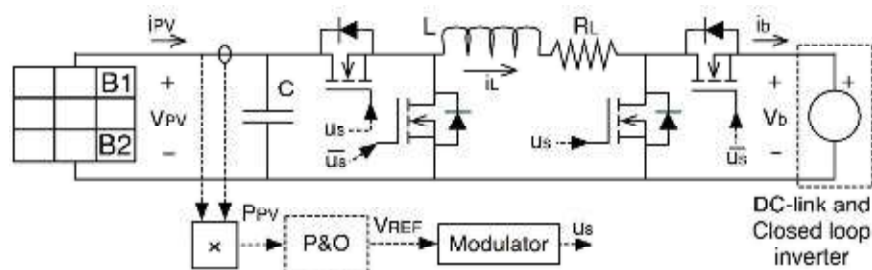


**Figure 6** MPPT system based on a Boost-Boost converter

**Efficiency comparison and considerations**

Considering a BP585 half module with  $I_{SC} = 5$  A,  $V_{OC} = 11.05$  V,  $V_{MPP} = 9$  V,  $I_{MPP} = 4.72$  A,

maximum power  $P_{MPP} = 42.48$  W, and a realistic  $R_L$  within  $[25, 250]$  mΩ, the efficiencies of the Boost, Buck and Buck-boost PV interfaces are depicted in figure 7(a), 7(b) and 7(c), respectively.

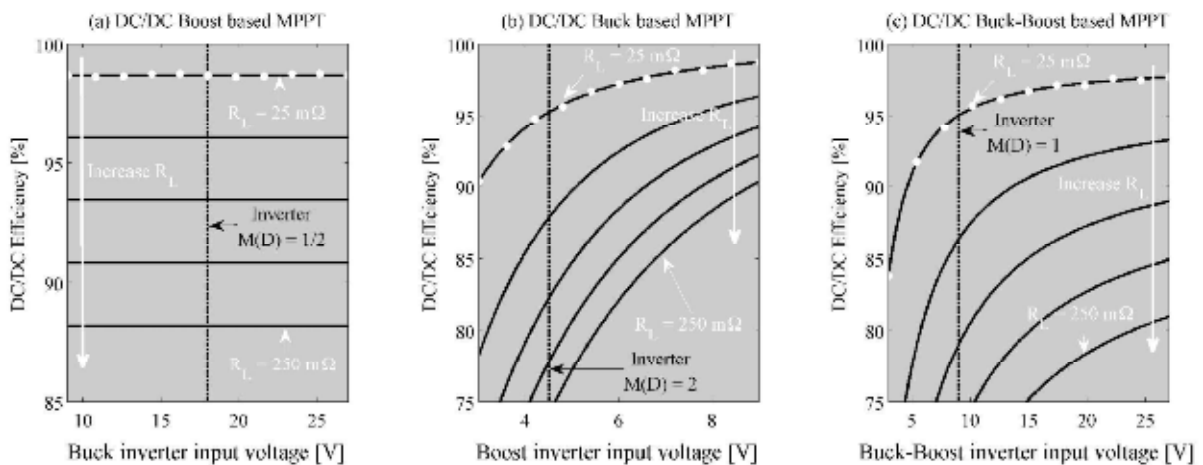


**Figure 7** Boost, Buck and Boost-Boost converters efficiency in MPPT systems

Since figure 7 analyses consider different DC-link voltages, different inverters must be adopted to provide the same grid voltage: in the Boost based MPPT a Buck inverter [4] is required, in the Buck based MPPT a Boost inverter is required [7], and in the Buck-Boost based MPPT a Buck-Boost inverter is needed [8]. To illustrate the analyses, 9 V peak-output voltage inverters are considered: for the Buck inverter it implies an input-output voltage relation  $M(D) = 1/2$ , or a duty cycle of 50 %; in the Buck inverter  $M(D) = 2$  corresponds to the same duty cycle; and in Buck-Boost PWM inverters a duty cycle of 50 % represents  $M(D) = 1$ . Therefore, the adopted DC/DC converters operating with the selected inverters are equivalent systems.

Figure 7 analyses show that the efficiencies of the Buck and Buck-Boost solutions depend on the adopted DC-link voltage, while the Boost solution has an almost constant efficiency. From such curves it is also concluded that the Boost solution is the most efficient one. To analytically verify such an hypothesis, the solutions power losses are normalized for the  $P_{MPP} = I_{MPP} \cdot V_{MPP}$  to define the losses factor  $\beta = P_{LOSS}/P_{MPP}$  for the Boost  $\beta_{BO}$ , Buck  $\beta_{BU}$  and Buck-boost  $\beta_{BB}$  cases

$$\beta_{BO} = \frac{R_L \cdot I_{MPP}}{V_{MPP}}, \quad \beta_{BU} = \frac{R_L \cdot I_{MPP}}{V_{MPP} \cdot D_{BU}^2}, \quad (8)$$

$$\beta_{BB} = \frac{R_L \cdot I_{MPP}}{V_{MPP} \cdot D_{BB}^2}$$

where  $\beta_{BO} < \beta_{BU}$  and  $\beta_{BO} < \beta_{BB}$  for the same condition because  $D_{BU} < 1$  and  $D_{BB} < 1$ , which confirms that the Boost interface is the most efficient. Similarly, at the same DC-link voltage  $D_{BU} > D_{BB}$  which leads to  $\beta_{BU} < \beta_{BB}$ .

### Mismatching phenomenon and distributed MPPT

In the experiments and simulations of figure 2(b) both PV modules exhibit the same irradiance

conditions, but in real applications some PV modules can be shaded [5] by external objects generating different short-circuit currents. This phenomenon, named *Mismatching*, can produce hot spots that degrade the PV panel, and commercial PV manufactures include bypassing diodes to reduce such effect [3]. In example, the BP585 has two bypass diodes as depicted in figure 8, and if a PV module is shaded, the associated diode is activated for  $i_1 > I_{SC1}$  or  $i_2 > I_{SC2}$ .

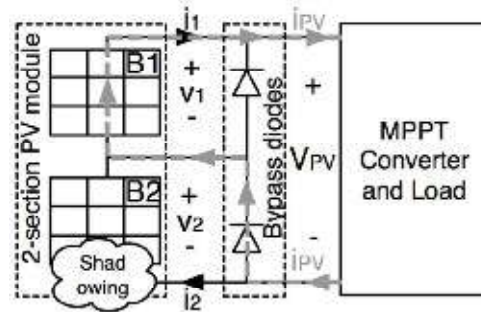


Figure 8 BP585 with coupled bypass diodes

Figure 9 presents the BP585 simulation for multiple mismatching conditions: a reference irradiance  $S_0 = 1000 \text{ W/m}^2$  was adopted, and the irradiance of the first and second modules,  $S_{M1}$  and  $S_{M2}$ , is given by the irradiance ratio  $\beta_s = S_{M1}/S_{M2}$ , where  $S_{M1} = K_{S1} \cdot S_0$  and  $S_{M2} = K_{S2} \cdot S_0$  with  $K_{S1} = [0.98, 0.96, 0.94, 0.92, 0.90, 1.00]$  and  $K_{S2} = [0.80, 0.60, 0.40, 0.20, 0.00, 1.00]$ .

It is noted that the first module exhibits a higher irradiance than the second one, which is eventually bypassed. Figure 9(a) also presents the activation of the second bypass diode when  $i_2 > I_{SC2}$ , producing power curves with two maximum points [3, 5]. In uniform conditions,  $\beta_s = 1$ , or with a module totally shaded,  $\beta_s = 0$ , the PV panel exhibits a single maximum. Moreover, the global maximum could be at the first or second peak depending on  $\beta_s$ , which could confuse the P&O controller. In addition, since the shaded PV module could be bypassed, there is not possible to extract the maximum achievable power  $P_{DMPP}$  represented by the sum of the modules  $P_{MPP}$ .

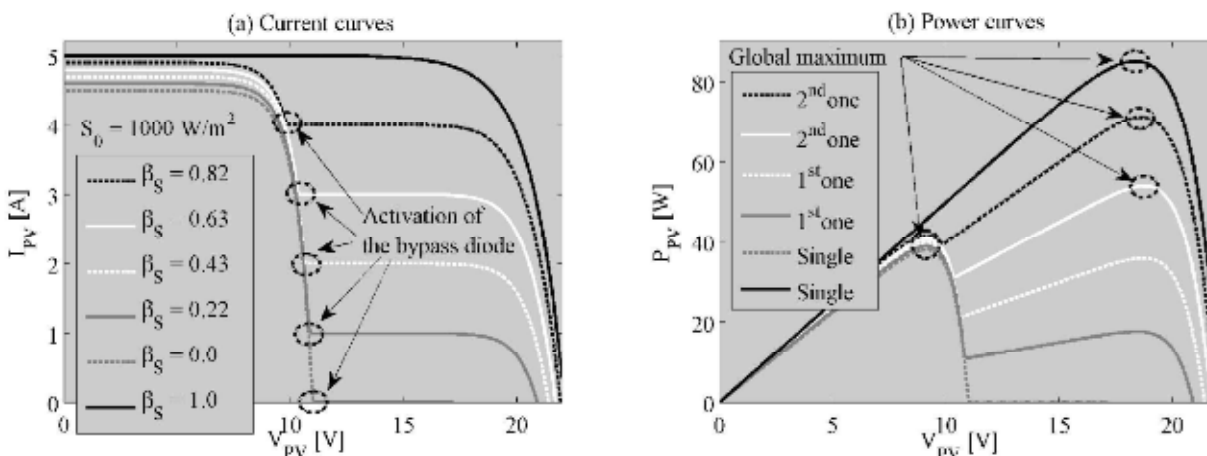


Figure 9 BP585 polarization curves in mismatched conditions

To obtain the  $P_{DMPP}$  each PV module can be associated to a DC/DC converter to extract all the  $P_{MPP}$ . Such a solution is known as Distributed Maximum Power Point Tracking or DMPPT [3]. Figure 10 describes the structure of a DMPPT solution based on classical DC/DC converters, where the DC/DC converters outputs are connected in series, but it is also possible to connect the converters outputs in parallel [5]. Figure 11 shows simulations on the same conditions of figure 9 but adopting a DMPPT solution, where a single maximum exists since there are no bypass diodes. Therefore, the DMPPT approach permits to extract the  $P_{DMPP}$  but the adopted DC/DC converters impact the output power since Boost, Buck, and Buck-Boost exhibit different losses.

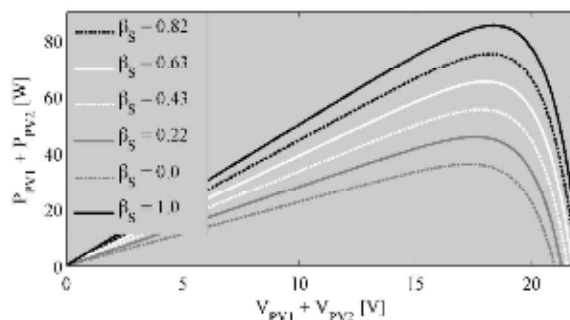


Figure 11 BP585 power curves in mismatched conditions using a DMPPT solution

The mismatching effect on the adopted two-module PV array can be also modeled by the difference between the modules MPP currents  $I_{MPP1}$  and  $I_{MPP2}$ , which can be related through a current factor  $k_i = I_{MPP2}/I_{MPP1}$ . Such a factor represents the level of mismatching between the two modules that is constrained within  $0 \leq k_i \leq 1$ , where  $k_i = 0$  corresponds to a single module totally shaded, while  $k_i = 1$  corresponds to uniform conditions. The power losses in the Boost  $P_{LOSS,BO2M}$ , Buck  $P_{LOSS,BU2M}$  and Buck-Boost  $P_{LOSS,BB2M}$  DMPPT solutions, under mismatching conditions characterized by  $k_i$  and  $\phi = R_L \cdot I_{MPP1}^2$ , are given by

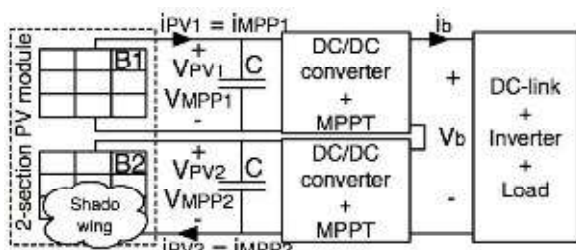


Figure 10 DMPPT solution based on classical DC/DC converters

$$\begin{aligned}
 P_{LOSS,BO2M} &= \phi(1+k_i^2), \\
 P_{LOSS,BU2M} &= \phi \left( \frac{1}{D_{BU1}^2} + \frac{k_i^2}{D_{BU2}^2} \right), \\
 P_{LOSS,BB2M} &= \phi \left( \frac{1}{D_{BB1}^2} + \frac{k_i^2}{D_{BB2}^2} \right)
 \end{aligned} \quad (9)$$

and the derivative of such power losses depending on the  $k_i$  are

$$\begin{aligned}
 \frac{d P_{LOSS,BO2M}}{d k_i} &= 2\phi \cdot k_i > 0, \\
 \frac{d P_{LOSS,BU2M}}{d k_i} &= 2\phi \left( \frac{k_i}{D_{BU2}^2} \right) > 0, \\
 \frac{d P_{LOSS,BB2M}}{d k_i} &= 2\phi \left( \frac{k_i}{D_{BB2}^2} \right) > 0
 \end{aligned} \quad (10)$$

where  $P_{Loss,BO2M}$ ,  $P_{Loss,BU2M}$  and  $P_{Loss,BB2M}$  are monotonically increasing functions, which means that the losses increase when the level of mismatching decrease, therefore the lower losses occur at  $k_i = 0$ , i.e. one module shaded; and the higher losses occur at  $k_i = 1$ , i.e. uniform conditions.

The efficiency comparison is analyzed by means of the losses factor  $\beta$ , which in this case depends on both power converters losses,  $P_{Loss,2M} = P_{Loss1} + P_{Loss2}$ , and on the total power generated by the array,  $P_{MPP,2M} = P_{MPP1} + P_{MPP2}$ . To simplify the expressions, the MPP voltages of both PV modules are considered equal,  $V_{MPP1} \approx V_{MPP2} \approx V_{MPP}$  which is an acceptable approximation as reported in figure 9(b). The losses factor for the DMPPT based on two Boost  $\beta_{BO2M}$ , two Buck  $\beta_{BU2M}$  and two Buck-Boost converters  $\beta_{BB2M}$  are given in (11).

$$\begin{aligned}
 \beta_{BO2M} &= \frac{R_L \cdot I_{MPP1}}{V_{MPP}} \cdot \frac{1+k_i^2}{1+k_i}, \\
 \beta_{BU2M} &= \frac{R_L \cdot I_{MPP1}}{V_{MPP}} \cdot \frac{\frac{1}{D_{BU1}^2} + \frac{k_i^2}{D_{BU2}^2}}{1+k_i}, \\
 \beta_{BB2M} &= \frac{R_L \cdot I_{MPP1}}{V_{MPP}} \cdot \frac{\frac{1}{D_{BB1}^2} + \frac{k_i^2}{D_{BB2}^2}}{1+k_i}
 \end{aligned} \quad (11)$$

It is noted that the Boost based DMPPT is the most efficient solution for any operating condition:

$$\begin{aligned}
 \forall \{D_{BU1} < 1 \wedge D_{BU2} < 1\} &\Rightarrow \beta_{BO2M} < \beta_{BU2M} \wedge \\
 \forall \{D_{BB1} < 1 \wedge D_{BB2} < 1\} &\Rightarrow \beta_{BO2M} < \beta_{BB2M}
 \end{aligned} \quad (12)$$

Finally, in mismatching conditions the DMPPT is more efficient than the classical bypass diodes solution, and in uniform conditions the bypass diodes solution is the more efficient since it does not introduce power losses while the DMPPT solution introduces its maximum power losses.

## Active bypass converter

The proposed active bypass (AB) converter is depicted in figure 12. It is based in two complementary operated MOSFETs, therefore the losses are collected in resistor  $R_L$  and the control structure is based on a multivariable P&O and a modulator. Moreover, the DC-link and closed-loop inverter are represented by a voltage source. Since the AB converter compensates the differences between the PV currents in mismatching conditions, no bypass diodes are required.

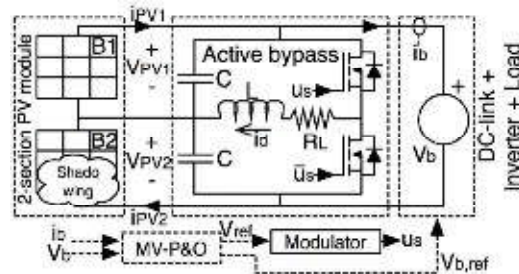


**Figure 12** DMPPT system based on the active bypass converter



In steady-state [6], the module voltages  $V_{PV1}$  and  $V_{PV2}$ , and the system output current  $I_b$ , are

$$\begin{aligned} V_{PV1} &= V_b \cdot (1-D) \quad \wedge \quad V_{PV2} = V_b \cdot D \quad \wedge \\ I_b &= I_{PV1} \cdot (1-D) + I_{PV2} \cdot D \end{aligned} \quad (13)$$

where  $D$  corresponds to the duty cycle,  $V_b$  to the AB output voltage, and  $I_{PV1}$  and  $I_{PV2}$  represent the modules currents. From equation (1), the PV module currents are given by  $I_{PV1} = I_{SC1} - A_1 \cdot \exp(B_1 \cdot V_{PV1})$  and  $I_{PV2} = I_{SC2} -$

$A_2 \cdot \exp(B_2 \cdot V_{PV2})$ , and the AB output current is calculated as

$$\begin{aligned} I_b &= [(1-D) \cdot I_{SC1} + D \cdot I_{SC2}] \\ &- \left[ \begin{aligned} &(1-D) \cdot A_1 \cdot \exp(B_1 \cdot (1-D) \cdot V_b) \\ &+ D \cdot A_2 \cdot \exp(B_2 \cdot D \cdot V_b) \end{aligned} \right] \end{aligned} \quad (14)$$

The power delivered by the AB is  $P_b = V_b \cdot I_b$ , where the second partial derivative of  $P_b$  is

$$\begin{aligned} \frac{\partial^2 P_b}{\partial V_b^2} &= -B_2 \cdot D^2 \cdot A_2 \cdot \exp(B_2 \cdot D \cdot V_b) \cdot [2 + D \cdot B_2 \cdot V_b] \\ &- B_1 \cdot (1-D)^2 \cdot A_1 \cdot \exp(B_1 \cdot (1-D) \cdot V_b) \cdot [2 + (1-D) \cdot B_1 \cdot V_b], \end{aligned} \quad 0 \leq D \leq 1 \Rightarrow \frac{\partial^2 P_b}{\partial V_b^2} < 0 \quad (15)$$

From (15) is it noted that the AB power-voltage curve exhibits a negative concavity for any duty cycle  $D$ , therefore there is always a single maximum that an external MPPT controller

is able to track. This is verified in figure 13, where uniform and mismatched conditions are considered, and optimum  $V_b$  and  $D$  values exist. Such a condition requires a multivariable P&O.

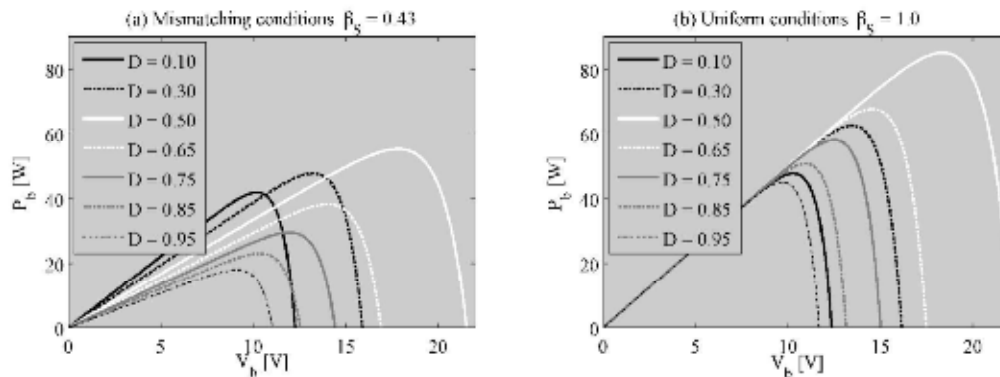


Figure 13 Power curves from AB-DMPPT solution for mismatching and uniform conditions

### AB converter regulation by means of a Multivariable P&O

It is noted that the AB converter duty cycle defines the difference between the PV voltages (13), i.e.  $V_{PV1} - V_{PV2}$ , then to define both PV voltages it is also necessary to set  $V_b$ , i.e.  $V_{PV1} + V_{PV2}$ . Therefore, both  $D$  and  $V_b$  must be optimized as reported in figure 13.

From figure 12 it is noted that the AB converter introduces losses due to  $R_L$ . This aspect has been addressed by optimizing the output power instead of the individual modules PV powers, which provides two advantages over traditional DMPPT approaches: first, it is required a single current sensor instead of dedicated current sensors for each PV modules [3]. Second, the DC/DC converter operating point is defined to

produce lower power losses. To optimize both D and  $V_b$ , the multivariable P&O (MV-P&O) algorithm given in figure 14 was adopted,

which perturbs one variable, i.e. D or  $V_b$ , and observes the perturbation effect on the output power.

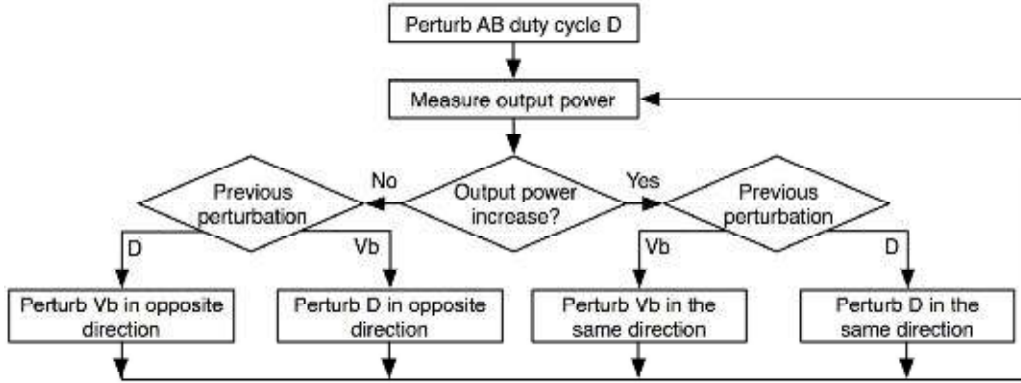


Figure 14 MV-P&O flowchart

**Efficiency of the DMPPT based on the AB converter**

From the steady state analysis of the AB converter of figure 12, the inductor current  $I_d$  is given by (16) if the MPP is ensured in both PV modules, while  $V_b$  fulfills the Kirchhoff law.

$$I_d = I_{MPP1} - I_{MPP2}, V_b = V_{MPP1} + V_{MPP2} \quad (16)$$

Since grid-connected inverters normally provide a  $V_b$  controller Gv, the condition given in (16) is achieved by generating Gv reference by means of MV-P&O, where the MV-P&O optimizes  $V_b$ .

To operate the AB on the MPP for both PV modules, AB duty cycle is given by (17), and the associated AB power losses are given in (18).

$$D_{AB} = \frac{V_{MPP2} + R_L \cdot I_d}{V_b} \quad (17)$$

$$P_{Loss,AB} = R_L \cdot I_{MPP1}^2 (1 - k_i)^2 \quad (18)$$

Since in the AB solution the inductor current is lower or equal than in the Boost case, a similar  $R_L$  is considered for the analysis. The derivative of (18) is given by

$$\frac{d P_{Loss,AB}}{d k_i} = -2R_L \cdot I_{MPP1}^2 \cdot k_i < 0 \quad (19)$$

which implies that the AB power losses are given by a monotonically decreasing function, whose maximum is obtained at  $k_i = 0$  that corresponds to the minimum losses in the Boost case for the same conditions (9)-(10). The minimum losses in the AB converter are obtained at  $k_i = 1$  condition, being near to zero. From (18) and (19) it is noted that the AB solution provides a trade-off between bypass diodes and classical DMPPT approaches: in mismatching conditions, i.e.  $0 \leq k_i \leq 1$ , the AB solution allows to track the global MPP as in the DMPPT; while in uniform conditions, i.e.  $k_i = 1$ , the AB system does not introduce power losses as the bypass diodes.

The efficiency comparison of the AB based DMPPT with the classical DMPPT is performed by means of the losses factor  $\beta_{AB2M}$ , which in this case depends on the AB power losses,  $P_{Loss,AB}$ , and on  $P_{MPP2M} = P_{MPP1} + P_{MPP2}$ . To provide a fair comparison, the MPP voltages of both PV modules have been considered equal, obtaining the  $\beta_{AB2M}$  in (20), which is always smaller than the Boost DMPPT losses factor (11), i.e.  $\forall k_i > 0 \Rightarrow \beta_{AB2M} < \beta_{BO2M}$ . Therefore, the AB solution is more efficient in uniform and mismatched conditions, but exhibits

the same efficiency when a PV module is totally shaded. Moreover, the relative losses factor  $\beta_{BO,AB}$  (20) confirms that the AB approach is more efficient than the Boost solution for any  $k_i > 0$  condition.

$$\beta_{AB2M} = \frac{R_L \cdot I_{MPP1}}{V_{MPP}} \cdot \frac{(1-k_i)^2}{1+k_i}, \quad (20)$$

$$\beta_{BO,AB} = \frac{P_{Loss,BO}}{P_{Loss,AB}} = \frac{1+k_i^2}{(1-k_i)^2}$$

Also, since the Boost solution is the most efficient option among the traditional DMPPT, the AB solution is a general improvement. But

the AB output voltage is equal to the sum of the PV voltages, therefore a Buck, Boost or Buck-Boost inverter is required to reach the grid voltage, which is similar to the bypass diodes approach.

Figure 15(a) plots the analyses given in (9), (18), and (20), which confirm that the AB solution is the most efficient one. In addition, it is also observed that the AB approach does not introduce power losses in uniform conditions, i.e.  $k_i = 1$ . Similarly, figure 15(b) depicts the  $\beta_{BO,AB}$  behavior, where it is noted that the AB power losses are smaller than in the Boost solution. Finally, equation (20) and figure 15 demonstrate the improved efficiency of the AB based DMPPT.

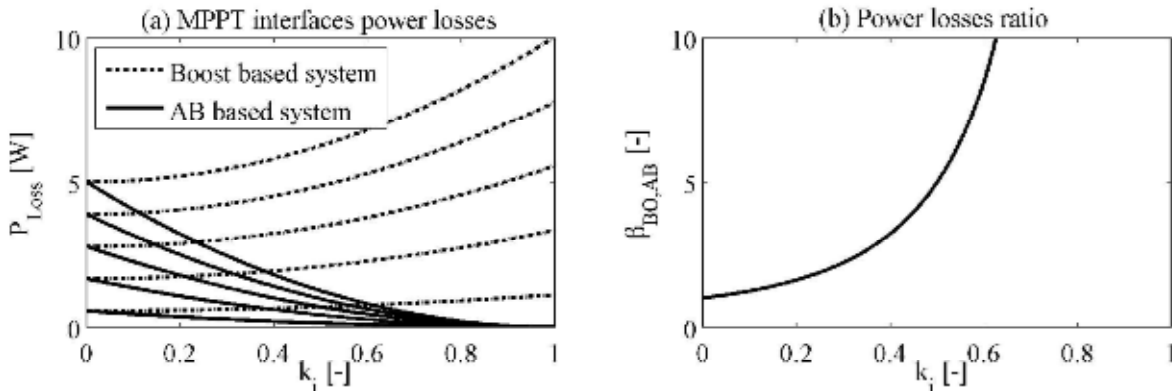


Figure 15 Efficiency comparison between AB and Boost DMPPT based solutions

### Simulation results

The previous analyses have been validated by means of simulations based on realistic and non-linear circuital simulations performed in the power electronics simulator PSIM. The simulations consider BP585 modules under the mismatched conditions given in figure 9 with  $\beta_s = 0.43$ ,  $\beta_s = 1.0$ , and  $\beta_s = 0.0$ . The simulations include the bypass diodes solution with a P&O algorithm, a Boost based DMPPT with the MV-P&O algorithm, and the proposed AB-based DMPPT with the MV-P&O algorithm. Finally, the simulations also consider the converters dynamics.

The simulations were carried out for dynamic irradiance conditions: from 10 ms to 20 ms the mismatched condition  $\beta_s = 0.43$  is imposed, then the uniform condition  $\beta_s = 1.0$  is present between 20 ms and 35 ms, returning to  $\beta_s = 0.43$  from 35 ms to 45 ms, and finally the second PV module is totally shaded  $\beta_s = 0.0$  from 45 ms. Figure 16 shows the simulation results, where in both DMPPT solutions the PV voltage of the first module is near the MPP voltage, which corresponds to the half of  $V_{MPP}$  reported in figure 2(b). But in such mismatched condition the bypass diodes operates at the second peak of the power-voltage curve of figure 9, imposing a large voltage. Similarly, the voltage of the second PV module reports that the three solutions follow the  $V_{MPP}$ . But from 45 ms,

when the second PV module is totally shaded, the DMPPT solutions drive to zero  $V_{PV2}$  because such a module does not produce power, while the bypass diodes takes more time to reach such a condition, wasting energy.

Moreover, the AB converter drives  $V_b$  to its optimal value for the mismatching level, while the bypass diodes P&O drives  $V_b$  to one of the power peaks. In uniform conditions both AB and bypass diodes impose the same DC-link voltage, where  $V_b = V_{MPP1} + V_{MPP2}$  is ensured. In addition, the voltage boosting of the Boost based DMPPT is illustrated by a larger  $V_b$ .

The simulations also report a high power production of the DMPPT solutions compared with the bypass

diodes. In addition, the AB solution produces higher energy than the traditional DMPPT for any mismatched condition: at  $\beta_s = 0.43$  the AB delivers 3.2 % more energy than the other DMPPT and 52.5 % more energy than the bypass diodes. Similarly, at  $\beta_s = 1.0$  the AB provides 5.2 % more energy than the typical DMPPT, while at  $\beta_s = 0.0$  the AB provides the same energy than the classical DMPPT. Such results confirm that the AB based DMPPT exhibits the best characteristics of both bypass diodes and classical DMPPT solutions: small losses at uniform conditions and global maximum power. Finally, for the 45 ms simulated, the AB produces 2670.6 J, while the Boost and bypass diodes solutions provide 2577 J and 1914.1 J, respectively.

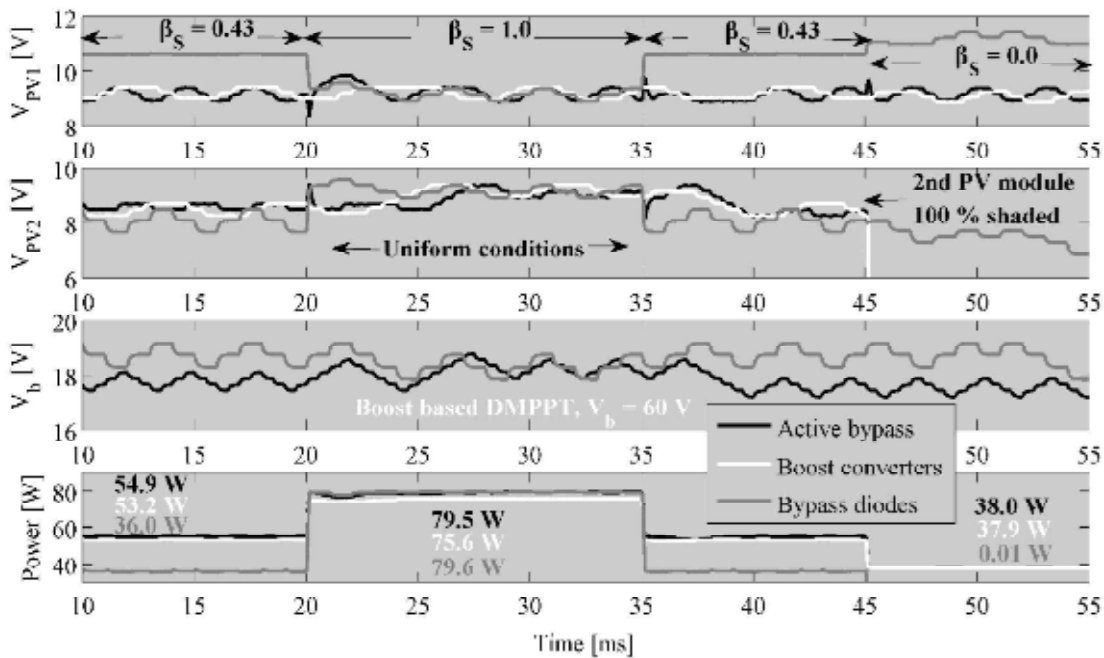


Figure 16 Dynamic simulations of the proposed AB solution, typical DMPPT and bypass diodes

### Conclusions

This paper proposes an active bypass structure to perform DMPPT. In comparison with traditional bypass diodes solution, under the same mismatching conditions, the AB solution provides higher power and exhibits similar power losses at uniform conditions. It has been demonstrated

that the AB system eliminates the multiple peaks condition that occurs in mismatching situations, therefore an external MPPT controller is able to reach the maximum power for any mismatching condition. Similarly, it has been demonstrated that AB based DMPPT systems produce lower power losses than solutions based on typical DC/DC converters.

## Acknowledgments

This work was supported by VECTORIAL-MPPT project of the Universidad Nacional de Colombia.

## References

1. N. Femia, G. Petrone, G. Spagnuolo, M. Vitelli. "Optimization of perturb and observe maximum power point tracking method." *IEEE Transactions on Power Electronics*. Vol. 20. 2005. pp. 963-973.
2. N. Femia, G. Petrone, G. Spagnuolo, M. Vitelli. "A Technique for Improving P&O MPPT Performances of Double-Stage Grid-Connected Photovoltaic Systems." *IEEE Transactions on Industrial Electronics*. Vol. 56. 2009 pp. 4473-4482.
3. N. Femia, G. Lisi, G. Petrone, G. Spagnuolo, M. Vitelli. "Distributed Maximum Power Point Tracking of Photovoltaic Arrays: Novel Approach and System Analysis." *IEEE Transactions on Industrial Electronics*. Vol. 55. 2008. pp. 2610-2621.
4. M. Fortunato, A. Giustiniani, G. Petrone, G. Spagnuolo, M. Vitelli. "Maximum Power Point Tracking in a One-Cycle-Controlled Single-Stage Photovoltaic Inverter." *IEEE Transactions on Industrial Electronics*. Vol. 55. 2008. pp. 2684-2693.
5. G. Petrone, C. Ramos. "Modeling of photovoltaic fields in mismatched conditions for energy yield evaluations." *Electric Power Systems Research*. Vol. 81. 2011. pp. 1003-1013.
6. R. Erickson, D. Maksimovic. *Fundamentals of power electronics*. Ed. Springer, 2<sup>nd</sup>, New York. 2001, pp. 11-50.
7. C. Albea, F. Gordillo, C. Canudas. "Adaptive control design for a boost inverter". *Control Engineering Practice*. Vol. 19. 2011. pp. 32-44.
8. C. Wang. "A novel single-stage full-bridge buck-boost inverter." *IEEE Transactions on Power Electronics*. Vol. 19. 2004. pp. 150-159.